

APPLICATION OF INSAR TECHNOLOGY IN GEOGRAPHICAL SITUATION MONITORING

WANG Yuhong¹, TIAN Qixia²

1.Yunnan remote sensing center, Kunming, China - 511611478@qq.com

2.BeijingSupermap Software Co., Ltd. Kunming office, Kunming, China - 1064861995@qq.com

KEY WORDS: InSAR, Geographical situation monitoring, D-InSAR, The terrain Deformation, Interference figure, Application

ABSTRACT:

In this paper, based on the geographical situation monitoring project of the earthquake zone of ludian county, zhaotong city, yunnan province, using the data of the radarsat-2 satellite(time frame is 20140304-20150416), InSAR technology is used to monitor the topography of the earthquake zone(about 420 square kilometers of monitoring area). **Through the analysis of topographic deformation results, the scope of the terrain change is obtained, and the application and problems of InSAR technique in topographic geomorphological monitoring are discussed.**

Corresponding author

Wang yuhong

1. INTRODUCTION

The synthetic aperture radar interferometry (InSAR) and the synthetic aperture radar differential interferometry (D-InSAR) are the rapid development of space to observe new technologies after the 20th century. Compared with traditional spatial remote sensing technology, synthetic aperture radar has full range the weather, full day, high resolution, the ability to penetrate the vegetation and the ground have some outstanding advantages, not only traditional method of photography measurement and remote sensing has been effectively complemented, and new observation methods and application fields have been developed. InSAR technology not only should surveying and mapping such as topographic mapping and DEM generation, it can also be applied to thematic mapping such as agriculture and forestry mapping. The monitoring of geographical situation is a major project developed by the country in recent years. The project has been applied to a number of high-tech technologies, such as GIS, GPS and RS technology. New space observation technology is developed in the late twentieth Century, InSAR technology will be further implemented in national-disaster monitoring projects. Based on the geographical situation monitoring project of the earthquake area of Ludian county in Zhaotong city, Yunnan province, this paper discusses application and encountered problems on the technique of InSAR monitored in the terrain and geomorphology.

2. MAIN BODY OF TEXT

2.1 Basic principles of InSAR

This section focuses on the basic principles of InSAR. The interference analysis of two SAR images in the same area obtained at different time/location can be understood as the co-conjugate of pixel complex values is multiplied, that is

$$IF(r, a) = M(r, a) S(r, a)^* \quad (1)$$

Here, (r, a) is the pixel slope, azimuth direction coordinates, M, S , respectively, main SAR image and

secondary image, and IF is obtained the interferogram (plural). As shown in FIG. 1, a conjugate multiplication actually implies a phase reduction of the corresponding pixel, that is

$$\phi = \psi_1 - \psi_2 \quad (2)$$

Therefore, the phase principal value of each complex number in the graph is dominated by equation (1), and the phase difference between the images corresponds to the pixel. That is the interference phase.

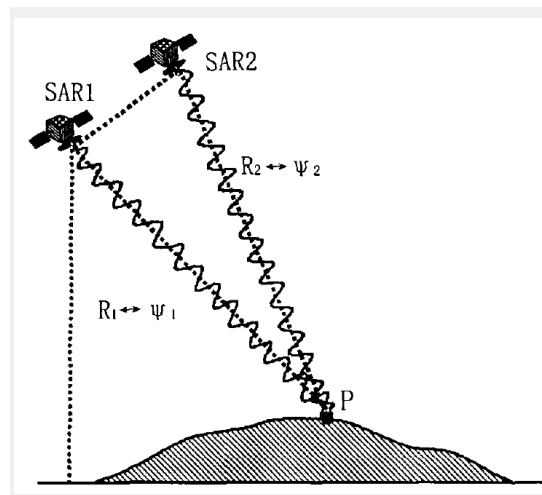


Figure 1 Basic principle diagram of InSAR

2.2 Data processing flow

2.2.1 The data clipping: The SAR data purchased is the data of the Canadian Radarsat-2 satellite, and the overall SAR data coverage is 125km x 125km, it is much larger than the required monitoring range (about 420 square kilometers of monitoring area), for the convenience of data processing and to reduce the amount of computation, you need to cut it to just cover the monitoring area. The data processing software uses GAMMA software of the Swiss GAMMA company Research and development.

2.2.2 Image co-registration: Because the two images in the InSAR are taken at different times and satellites posture, the pixels between them are not corresponding to each one, the pixel point registration is required, which is to calculate the reference image (the main image) and the registration (the secondary

image) the relationship between Azimuth and distance (Range) is used to use this relationship to treat the registration image row coordinate transformation and resampling.

FIG. 2 shows the intensity of image interference in the main image (a) and the secondary image (b) after registration .

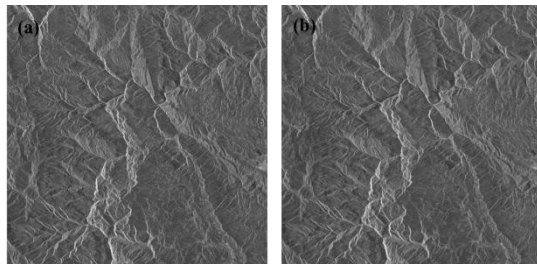


Figure 2 The intensity diagram of the main image (a) and the secondary image (b) (after registration)

2.2.3 Generated interference pattern: The multiple conjugate multiplied from the image and the main image after the resampling is multiplied to produce a complex interferogram. In order to evaluate the interference phase quality, at the same time, a coherent coefficient diagram corresponding to the interference phase diagram is generated while generating the interference phase diagram (FIG. 3). In terms of the effect of computer display, the purple region in the figure shows the region with high coherence, and its interference phase striation is clear, interferometric phase observation is reliable; In contrast, a large area of cyan area indicates a region with low coherence and its interference phase is affected by noise. The interference phase is seriously affected by the noise, and the observation quality is low.

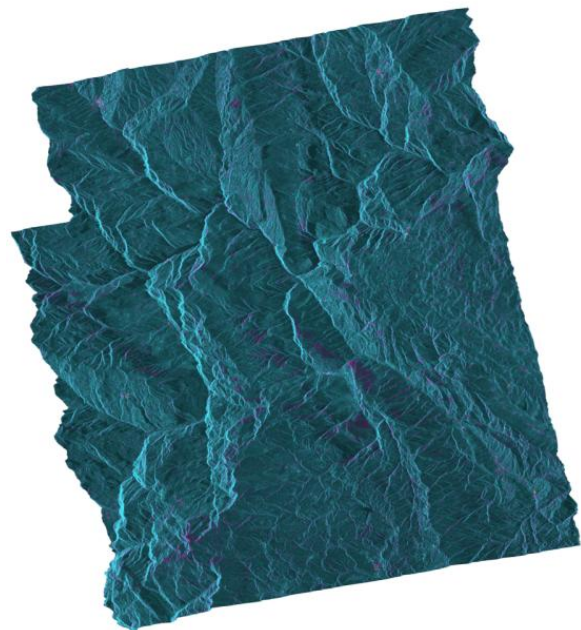


Figure 3 Original coherent graph



Figure 4 Differential interference pattern

2.2.4 Remove ground and topographic phase: The flatland effect refers to the change of the phase of the flat phase in the interference fringes with the change of distance and orientation the phase of the change. It is mainly affected by the geometry of SAR system, such as platform height, the lower Angle of antenna and baseline length the effect of the element. In addition to the flat phase, the original interference fringe pattern includes the topographic phase. The topographic phase is based on the monitoring area the fluctuation is caused by the inverse ratio of the radar wavelength and radar to the ground distance, which is proportional to the vertical baseline and the terrain height. In order to score from the deformable phase, you must remove the flat and topographic phase. For this reason, the external DEM data can be used for flat and topographic phase the simulation of bits is then subtracted from the original phase to form the differential interference graph (shown in figure 4).

2.2.5 Phase filter: Because the generated InSARinterferogram is caused by geometric overthrust, system thermal noise, time change and local match misalignment, the influence of the incoherent noise and other factors, signal-to-noise ratio of the generated InSARinterferogram is low and needs to be filtered and processed in this paper, the signal-to-noise ratio of the interference graph is improved, and the reliability of the phase solution and the interpretation ability of the interference graph are further improved. Figure 5 shows the following the interferogram (a) and the coherent graph (b) after the complex image filtering. Compared to figure 4 and 5, the coherence value and phase value of the filter are available, there was a marked improvement in readability.

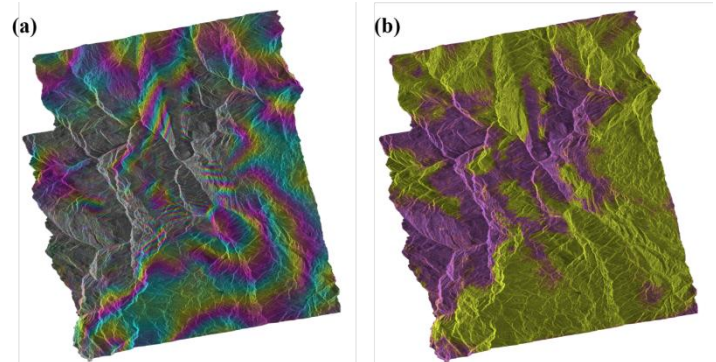


Figure 5 The differential interferogram graph (a) and coherence graph after filtering(b)

2.2.6 Phase unwrapping: Because of the generated phase interference graph, each pixel has the problem of the fuzzy degree of the phase, which is extracted from the interferogram, is actually the main value of phase, its value in the range of $\{-\pi, \pi\}$ in between. In order to get a real phase difference, You have to add an integer multiple of 2π to this range. Phase unwrapping is especially an important step in InSAR treatment, the quality of the final data product of InSAR is directly affected by the quality of the phase solution. Figure 6 is the least used the interferometric phase of the phase unwrapping is carried out.

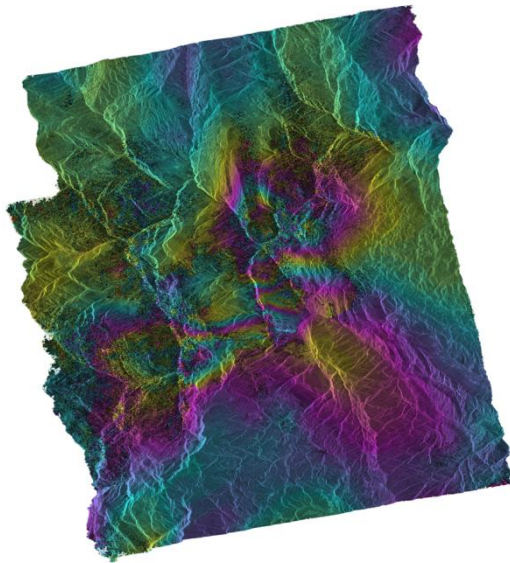


Figure 6 Interference phase diagram (after phase unwrapping)

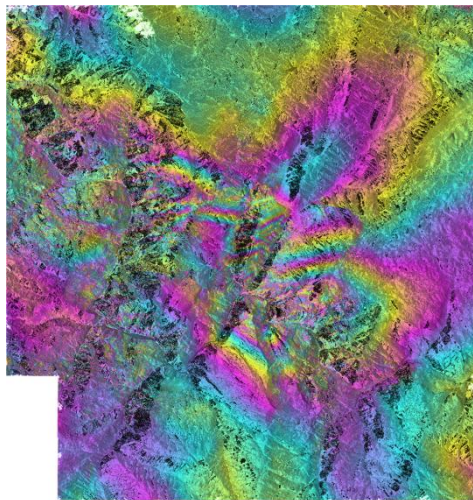


Figure 7 Map of deformation (after geocoding)

2.2.7 Geocoding: The resulting phase is in the radar coordinate system (line number, column number, elevation), and it needs to be converted to the right Angle coordinate system (longitude, latitude, elevation) of an ellipsoidal coordinate system, it can be used by us, namely, geo-coding processing. Figure 7 for the deformation diagram after the geocoding.

2.3 Analysis of topographic deformation results

The deformation results obtained by the interference of image are shown in figure 8, where the red pentagonal star is the epicenter location and the black curve is the monitoring range, the red curve is the area

of deformation area and the brown solid line is the position of the profile line. From FIG. 8 analysis, two distinct areas of surface change have been created due to ludian earthquake, one located at the northwest corner of the epicentre (line AA' location) and one located at the epicenter of the earthquake south east corner (line BB' location). The deformation of the northwest corner is mainly the subsidence, the maximum subsidence of about 16cm, the deformation area is close to 100 km². The deformation of the southeast corner mainly shows up as an increase, the maximum increase is about 15cm, and the deformation area is close to 85 km². In addition, some 50km² subsurface subsidence occurred in the northeast corner of the epicenter. These three surface changes were in August 2014. The results of the magnitude 6.5 earthquake and its aftershocks have been the most damaging.

In order to further show the magnitude of the deformation, the deformation values of double AA' and BB' in figure 8 are extracted, as shown in FIG. 9. FIG. 9 shows that the shape variable of the deformation area of AA' and BB' shows the large distribution of the middle and the line, contrary to the deformation of AA' and BB', this phenomenon is consistent with the deformation caused by the earthquake.

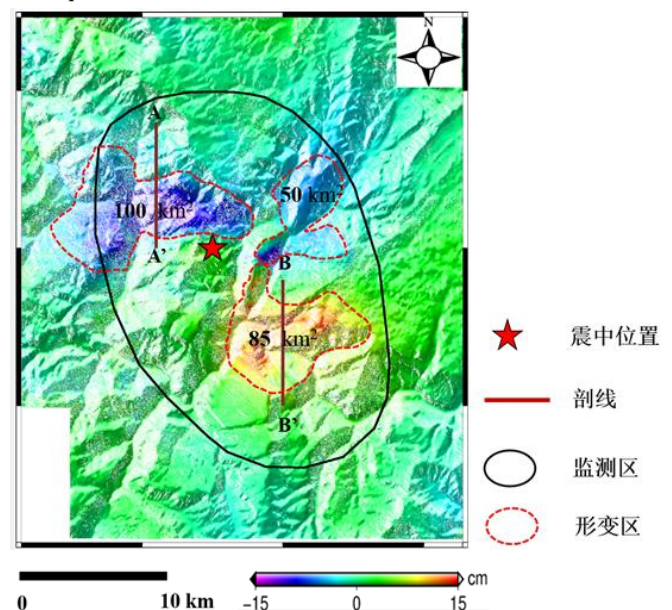


Figure 8 Deformation figure

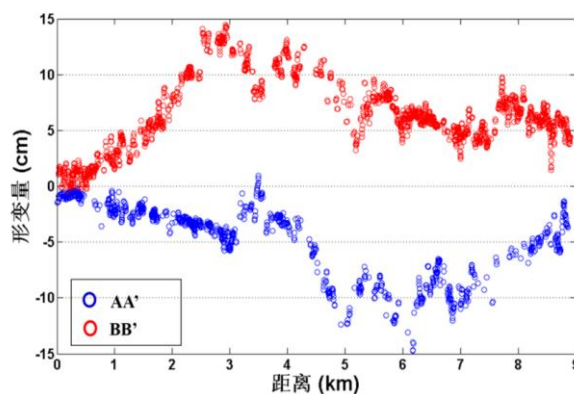


Figure 9 Profile deformation value distribution diagram

3. CONCLUSIONS

In this project, landslides and quake lakes caused by earthquakes are not reflected in the results of topographic deformation, which is because InSAR technology also has some limitations in the area of large change. Specific reasons are as follows:

Loss of time coherent. The precondition of the interference of two SAR images is to maintain a property of the earth's surface during the observation period. If the two SAR images are too long and the properties of the land change significantly (such as changes in crops and vegetation), it can cause time to lose coherence. Image interference

(20140304-20150416) is close to one year, during this period. The ground objects of the subsurface can change significantly, which can cause time loss.

Maximum detectable deformation capability. In the case of InSAR technology, the same resolution unit is seen during imaging, in more than half a wavelength, these deformations cannot be recovered from the InSAR interferogram, which is the maximum detectable deformation capability. During the monitoring period of this project, the deformation of the larger surface of the earth, such as landslide, collapse and barrier lake, etc., is in the interferogram. The expression is incoherent, unable to recover its deformation.

Geometric incoherence. Geometric incoherence mainly

refers to the overlapping and shadow of the monitoring area, such incoherent and topographic conditions. SAR imaging geometry is concerned. The monitoring area of this project is large, the SAR imaging geometry is single, and the geometrical incoherence is seriously affected.

Interference with other error items. Due to limitations of project data sources, it is inevitable to be exposed to the atmosphere during the process of obtaining deformation, the influence of delay, orbital error and phase unwrapping error affects the accuracy of the final deformation.

In order to obtain reliable deformation results, it is recommended to improve the data acquisition, image registration and phase solution. In addition, the method of observation is improved, such as the installation Angle reflector in the area with large surface change, to improve the coherence of the data.

4. REFERENCE

- LIU Guoliang, DING Xiaoli, CHEN Yongqi. The potential space to observe the new technology - synthetic aperture radar interference [J]. Earth science progress, 2000.
- LI Zhenhong, LIU Jingnan, XU Caijun. Error analysis in InSAR data processing [J]. Journal of wuhan university (information science), 2004.
- LIU Guoxiang, DING Xiaoli, LI Zhilin. Space registration of satellite SAR complex image [J]. Journal of surveying and mapping, 2001.
- HE Ping, XU Caijun. Study on the influence of satellite orbital error on SAR interference processing [J]. Journal of Geodesy and geodynamics, 2009.
- XU Caijun, WANG Hua. Comparison and error analysis of InSAR phase unwrapping algorithm [J]. Journal of wuhan university (information science), 2004.

- Suksmono A B. Adaptive Noise Reduction of InSAR Image Based on a Complex2Valued MRF Model and Its Application to Phase Unwrapping Problem. IEEE Trans.Geosci. Remote Sens , 2003 ,41(3) : 699~709.
- Dixon T. SAR Interferometry and Surface Change Detection.<http://PPsouthport.jpl.nasa.gov/scienceapps/dixon/index.html> ,2003.
- GoldsteinR. Atmospheric Limitations to Repeat-track Radar Interferometry. Geophys. Res. Lett , 1995 , 22 (18) : 2517~2520.
- Ding, x. L. , G. X. Liu, Z. W. Li, and Y. Q. Chen, Ground subsidence monitoring in Hong Kong with satellite SAR interferometry[J]. Photogrammetry Engineering&RemoteSensingVol. 70,No. 10,PP. 1131—1137,2004.
- MassonnetD , Feigl K L. Radar Interferometry and Its Application to Changes in the Earth's Surface. Rev.Geophys. , 1998 ,36 (4) :441~500.